Quasi-Static, Impact and Energy Absorption of Internally Nested Tubes Subjected to Lateral Loading

A. Baroutaji[1], M.D. Gilchrist[2], D. Smyth[3], A.G. Olabi[3]

(1)- School of Mechanical and Manufacturing Engineering, Dublin City University, Glasnevin, Dublin 9, Ireland.

(2)- School of Mechanical & Materials Engineering, University College Dublin, Dublin 4, Ireland

(3)- Institute of Engineering and Energy Technologies, School of Engineering, University of the West of Scotland, Paisley, PA1 2BE

Abstract:

This paper presents the responses of nested tube systems under quasi-static and dynamic lateral loading. Nested systems in the form of short internally stacked tubes were proposed as energy absorbing structures for applications that have limited crush zones. Three configurations of nested tube systems were experimentally analysed in this paper. The crush behaviour and energy absorbing responses of these systems under various loading conditions were presented and discussed. It was found that the quasi-static and dynamic responses of the nested systems were comparable under an experimental velocity of v=4.5 m/sec. This is due to insignificant strain rate and inertia effects of the nested systems under the applied velocity.

The performance indicators, which describe the effectiveness of energy absorbing systems, were calculated to compare the various nested systems and the best system was identified.

Furthermore, the effects of geometrical and loading parameters on the responses of the best nested tube system were explored via performing parametric analysis.

The parametric study was performed using validated finite element models. The outcome of this parametric study was full detailed design guidelines for such nested tube energy absorbing structures.

Keywords: Nested tubes, Energy absorbing systems, lateral collapse, ANSYS-LSDYNA, Quasi-static loading, Dynamic loading.

1 Introduction:

The function of energy absorbing structures is to minimise injuries to human beings and to protect vital structures from impact damage or any other dynamic loads. The design and development of these systems require study and understanding of materials engineering, structural mechanics, impact mechanics, and the theory of plasticity. The behaviour and response of energy absorption structures under dynamic loadings such as the impact loading, is considered to be a very important field for design and research engineers who are involved in the automobile, aircraft, spacecraft, and nuclear industries. Thin-walled tubes of different geometry and materials are commonly used to absorb kinetic energy through plastic material deformation. Over the last four decades, a significant amount of research has been conducted on the energy dissipated by thin-walled tubes. The main findings were outlined and presented in a review article by Olabi et al. [1], Alghamdi [2], and Abramowicz [3]. General information and discussion about energy absorption structures and materials can be found in books by Lu and Yu [4] and Jones [5].

Many applications employ thin walled tubes as energy absorption devices such as thin walled tubes at the front of passenger trains and vehicles, aircraft sub floor structures, and thin-walled tubes at the base of lift shafts.

Thin-walled tubes can absorb kinetic energy as a result of many types of deformation, leading to various energy absorption responses. The principle ways of destroying tubes include lateral compression [6-17], lateral indentation [18-27], axial crushing [28-37], tube inversion [38, 39], and tube splitting [40-45].

The axially loaded tubes have been widely used as energy absorbing devices and have received considerable amount of attention due to the fact that these structures have high energy absorbing capacities and stroke length per unit mass. In spite of these superb features, the axially crushed structures still experience certain drawbacks, such as very large fluctuations of the collapse load about a mean load, and the unstable deformation mode termed as global bending deformation mode which restrict their use in all energy absorption applications.

The energy absorbing capacity of laterally flattened tubes was found to be greater than that of lateral indentation, but not as much as for axial crushing.

Laterally loaded tubes have a distinct advantage over tubes compressed axially due to fact that the bending collapse mode generated from lateral loading result in a smooth force-deflection response. Also, the laterally loaded tubes do not undergo any kind of unstable deformation mode even under the off-axis loading. However, the deformation mode of these structures is plastic bending at plastic hinges. This deformation mode results in plastic strains localisation around the plastic hinges and makes the dissipation of energy through the lateral collapse inefficient.

Therefore, to overcome the aforementioned drawback and to enhance the energy absorbing capacity of single empty tubes, foam-filled components [46-48] and nested tube systems have [49-53] been proposed.

Much of the research on the laterally crushed energy absorbers has focused on those which are empty or foam filled components. However, the nested tube systems, which consist of more than one component, have received less attention.

In the present study, nested tube systems using internally stacked groups of circular and oblong tubes have been proposed as energy absorbers. These systems are of particular importance for applications that are restricted in terms of space and with a limited crush zone. Three different configurations were analysed, all of which had

deformable tubes arranged so that they deformed synchronously upon loading, in order to achieve the desirable force-deflection response. The quasi-static and dynamic responses of these systems were investigated. A series of experiments were carried out by using Instron instrument for the quasi-static loading and Zwick Roell machine for the dynamic loading. The effect of geometrical and loading parameters on the energy absorption behaviour and deformation modes of these systems was examined numerically by using finite element analysis.

2 Experimental Work

2.1 Material properties and specimens

Mild steel tubes were used for manufacturing the samples. The tubes were drawn over a mandrel (DOM), cold finished and manufactured according to the DIN standards, DIN 2393 ST 37.2. The chemical composition of the steel used in this work is displayed in Table 1. Tensile tests were carried out in order to determine the mechanical properties of the tubes as shown in Figure 3. Dog bone samples (tensile samples) were prepared by flattening the tube and cutting the specimens. Figure 3 displays the true stress-strain curves of the tensile sample. Upon examination of this figure, it can be seen that the stress-strain curve displays unusual behaviour in which strain softening occurred almost immediately after yielding with no evidence of strain hardening. This phenomenon is due to sample necking which takes place immediately after yielding. This behaviour is termed tension instability and the cold rolling process might be the reason for this. In addition, the method of preparing tensile samples might also have an effect on the stress – strain behaviour of the tensile sample.

Table 2 shows the mechanical properties of the mild steel material derived from the true stress-strain curve. The yield stress is validated according to DIN standards, which state that the yield stress of this material is within the range of 450–525MPa [51, 52].

Table 3 summarizes the geometry profiles and the dimensions of all nested tube systems used in this work.

2.2 Experimental set-up

For the quasi-static loading, The Instron Model 4204 testing machine was used to perform the quasi-static experiments on the respective specimens. The loading frame comprises of two vertical lead screws, a moving crosshead and an upper and a lower bearing plate. The maximum capacity of this loading frame is 50 kN. The loading force is measured by a loading cell which is attached to the moving crosshead of the loading frame. This load cell is comprised of multi strain gauges. The gauges are connected as a Wheatstone bridge, so any unbalance in this bridge is recorded as voltage. This voltage is then used to indicate the amount of force applied to the samples. A CPU is used as control unit to control movement of the crosshead. This control unit also provides the data acquisition and data readout from the loading frame. Instron 4204 series software is integrated to display the results. Many parameters such as displacement, load, strain and energy can be obtained. A prescribed velocity of 10 mm/min was applied to the moving crosshead of the instrument to ensure that there were no dynamic effects. Many researchers [47,48] used velocities between 0.5 and 15 mm/min in the quasi-static lateral compression tests. The quasi-static test set- up for the nested tube sample is shown schematically in Figure 1.

The Impact testing of the various samples was conducted using the Zwick Roell 5HV series (Figure 2). The load-time response, during the impact event, was captured by using a Kistler 9091 series piezoelectric force transducer which has a maximum load capacity of 250 kN. The transducer was mounted on the moving carriage and attached to a striker by a lock-unlock mechanism. The maximum drop height is 1.2 meters. The impact mass, which consists of a striker mass and a carriage mass, slides vertically along the guide rails. The initial velocity of the striker (impact velocity) was captured by a photo gate arrangement which is comprised of photo diodes passing through a flagged gate. Figure 2 displays the Zwick Roell impact testing machine with an explanation of striker mass and sample positions.

Rosand IFW (Intelligent Free Wheel) V 1.10 was employed as a data acquisition system. This system has a maximum frequency response rate of 670 kHz and a total data point capture of 4000. The system software obtains signals from the force transducer and records the force measurements with respect to time. The software is equipped with a filter option, which is based on the second order Butterworth filter.

During the experiment, the samples were fixed in their position by using a simple fixture. The striker was set in motion by selecting the velocity of impact and hence the drop height and the energy absorption were calculated by the machine software. The total impinging mass consisted of the striker mass and the carriage mass. The appropriate drop height was adjusted automatically by the machine by setting the zero position and the velocity of the striker. For each sample tested, a frequency of 1000Hz and a total of 100 data points were selected to collect data from the transducer.

2.3 Experimental results and discussion

2.3.1 Quasi-static responses

The quasi static responses of the nested tube systems were investigated for many reasons. First, the experimental setup for quasi-static loading is relatively simple compared with that for a dynamic loading test. Second, the energy absorption responses and deformation mode of structures under a low impact velocity are very similar to those obtained with quasi-static loading. Third, it is very important to compare the dynamic results against quasi-static results so that the effect of dynamic loading can be determined and quantified.

2.3.1.1 NTCO system

Figure 4 shows the force and energy responses of the NTCO system, and Figure 5 shows the deformation history of NTCO system. Originally, this system consisted of two different circular tubes with a gap between them. This gap allowed the two components to deform sequentially as loading proceeded, hence it caused a non-monotonic rise in force throughout the deformation stroke. In previous studies carried out by Olabi et al. [51, 52], two cylindrical spacers were inserted between the gaps of the tubes to eliminate a non-monotonic increase in force as contact was established between the tubes. In this system (NTCO), the gap between the tubes was eliminated by elongation of the internal tube which changed its profile to oblong. Using oblong tubes instead of circular tubes had two aims: firstly, to eliminate the non-monotonic increase in force, and secondly, to reduce mass as in other systems the cylindrical spacers used to fill the gap increased the mass of the system. Upon examination of the force-deflection response of the NTCO (Figure 4), it can be seen that the force increased linearly up to its characteristic ‘collapse’ load,

followed by a slight strain hardening behaviour in the post collapse stages. The strain hardening behaviour of this system at the early stages of plastic deformation seemed to be negligible. This phenomenon is due to the use of a combination of two different profiles (ie: circular & oblong) that have contrary hardening behaviours. At approximately 50 mm deflection, the force started to rise again. This is due to the 'bottoming out' of the oblong tube. This can be avoided by simply applying a slightly shorter displacement stroke. It was noticed that the force response up to 50 mm deflection was almost rectangular in shape, which is a very desirable feature in energy absorption systems. As a result of obtaining this rectangular shaped response, the corresponding energy absorption response was almost linear for the entire deflection stroke. The deformation history of the NTCO is presented in Figure 5. Upon observation of the collapse mode history, it can be seen that the system exhibits a symmetrical mode of collapse at all stages and the two components of the system deformed simultaneously.

2.3.1.2 NTDC system

The NTDC system consists of two small tubes placed inside one large tube; the internal tubes have different diameters and the same thicknesses. The energy and force responses of the NTDC system are depicted in Figure 6, with the various stages of deformation of a typical sample shown in Figure 7. In the range up to 70 mm deflection, the force response of the NTDC had a rectangular shape. The small tube was not deformed at this stage and worked as a cylindrical indenter for compression of the other internal tube. This rectangle response is due to a combination of strain hardening of the outer tube which was compressed by a flat plate indenter, and strain softening of the internal large tube which was compressed by the small internal tube. Once the large tube collapsed and was completely destroyed (at approximately 70

mm deflection), the small internal tube started to deform causing an increase in the force values of up to 27.5 [KN], following which the whole system starts to strain harden up to the end of the compression process. The test was stopped at a deflection of 90 mm, in case the significant increase in the load might cause harm to the testing instrument. From the various stages of the deformation profile of the NTDC presented in Figure 7, it can be seen that the system exhibits an asymmetric collapse around the horizontal axis, while it collapses symmetrically around the vertical axis. The asymmetrical collapse mode is due to the fact that two components of the system (the large tubes) deformed simultaneously at the beginning of the collapse, while the smaller tubes deformed at the very end of the compression process.

2.3.1.3 NTSC system

Generally, for an effective energy absorbing structure, the system components need to deform simultaneously. To apply this concept, the different sized circular tubes of the NTDC were replaced by same sized tubes. The internal tubes had the same thicknesses and same diameter and were manufactured from the same material. Theoretically, when a compression load is applied to the NTSC system, the three components (outer large tube & internal small tubes) should deform at the same time. Figure 8 displays the experimental responses of the NCST system along with the various stages of deformation in Figure 9. Upon examination of Figure 9, it can be seen that a symmetrical collapse mode was not achieved, and neither was the simultaneous deformation of the three components. One possible reason for this phenomenon may be the difficulty of getting two tubes that are exactly the same for the internal components. It was therefore concluded that the NTSC system was more sensitive to geometrical imperfections, with any small difference between the internal tubes resulting in the collapse of one tube before the other. From the force

response of the NTSC shown in Figure 8, the strain hardening rate is higher than that noticed in the NTDC, as the internal tubes are of the same size. A slight rise in force was noticed at a deflection of 55 mm. This rise was due to the collapse of the second internal tube and the self-contact of the first internal tube. At approximately 75 mm of deflection, the system starts to experience a significant increase in force up to the end of the compression process. This increase is due to the material strain hardening that occurred in the three tubes, which led to a greater overall force required to compress the system.

2.3.2 Impact responses

In real-world energy absorption applications, the structure is mainly subjected to dynamic loading such as Impact. Thus the responses of nested systems under lateral impact loading are addressed in the this section

2.3.2.1 NTCO system

The dynamic load-deflection response of NTCO was very close to its quasi-static counterpart, as can be seen in Figure 10. This indicates the insignificant role of strain rate and inertial effects on the dynamic response of the system under the given applied velocity of the striker. The initial and final deformed stages of the NTCO system under dynamic loading are plotted in Figure 11. From this figure, it can be observed that the final deformed profile of the system under the quasi static and dynamic loading conditions are very similar. In general, the energy dissipated by the lateral collapse of the thin walled components is localised around the plastic hinges which were formed during the collapse. Taking into account the similar deformation modes of NTCO under various loading conditions, the amount of dissipated energy by the NTCO under both conditions was similar.

2.3.2.2 NTDC system

The quasi-static and dynamic force deflection response of NTDC is presented in Figure 12. Due to the presence of the clamping bar in the dynamic test, the full collapse of the large inner tube was not achieved. At approximately 49 mm of deflection, the small inner tube started to collapse causing a rise in the dynamic force. Apart from the geometrical difference between the quasi-static and dynamic tests due to the need for clamping the absorbing system, the crushing strengths of the systems under both loading conditions were very similar. This is evidence of the insignificant role of the dynamic effects on the system response under test impact velocity. Also, as evidence of the negligible role of the inertia effects for the given test velocity (v=4.5 m/sec), the deformation profile of the system was plotted in Figure 13. It can be seen that the final deformation profile of the system under dynamic loading is very similar to that of quasi-static loading, particularly if the symmetric collapse mode of the large outer tube is taken into consideration.

2.3.2.3 NTSC system

The load-deflection curves of the NTSC system under quasi-static and dynamic loading conditions are shown in Figure 14. The dynamic results are for an impact velocity of 4.5 m/s. The initial and final stages of the deformation under impact loading are presented in Figure 15. From Figure 14, it can be seen that the dynamic force-displacement response is very similar to its quasi-static counterparts. The close responses of the NTSC under quasi-static and dynamic loadings demonstrate that the strain rate and inertial effects for the given applied velocity of the striker are almost negligible.

Upon examination of the deformed profiles of the NTSC (Figure 15), it can be clearly seen that the three components of the system have been crushed simultaneously and an almost symmetrical collapse mode was obtained.

2.4 Energy absorption characteristics

The performance of energy absorbing systems can be evaluated by means of several criteria. Some useful indicators were proposed by Thornton et al. [20], such as crush efficiency, energy efficiency, specific energy absorption capacity, and weight effectiveness. The specific energy absorption capacity is the most important characteristic of energy absorbers. SEA is defined by energy absorbed per unit mass, and is given by:

$$\mathrm{SEA} = \frac{\mathrm{E}}{\mathrm{m}} \qquad (1)$$

Where m is the mass of the energy absorber. E is the energy absorption capacity which can be measured by calculating the area under the force-deflection response of an energy absorbing device. The energy absorption capacity can be defined as the integration of a load-displacement curve as follow.

$$\mathrm{E} = \int_0^{\delta} \mathrm{F}(\delta)\,.\,\mathrm{d}\delta \qquad (2)$$

Where δ is the displacement, and F (δ) is the load-displacement response.

The stroke efficiency is defined as the stroke length divided by the characteristic length of a structure, such as the outer diameter or the original length. The stroke efficiency for lateral collapse of a nested system tube can be defined by the equation

$$e_g = \frac{\delta}{D} \quad (3)$$

Where D is the diameter of the main tube in the nested system. e_g is considered as a good indicator for describing the amount of material that can be used during the collapse. All nested systems studied in this paper were crushed up to their 70% of their original diameter to avoid the system overload that may cause the tubes to fracture or might cause harm to the testing instrument.

The energy efficiency indictor is given by

$$e_E = \frac{E}{F_{max} * L} \quad (4)$$

Where F_{max} is the maximum load observed in the force-displacement response, and L is the original length of the absorber. It is recommended to maximize the energy efficiency of the energy absorber. Ideally, to achieve the maximum value of e_E, the force-displacement response of the energy absorber should be a rectangle response.

The work effectiveness is a combination of the specific energy absorption capacity and the crush efficiency indicator, and it is defined as follow:

$$W_{eff} = SEA \times e_g \quad (5)$$

This indicator is a very useful one, particularly in structures that are restricted in terms of both weight and space.

The last indicator used to compare the energy absorption performance of nested systems is the energy absorbed per unit crush length (E_{cl}) which can be calculated

using the absorbed energy (E) divided by the undeformed length of the absorber. This indicator is a very important one in applications that have a limited crush zone. For energy absorbers crushed laterally the E_{cl} can be formulated as follow.

$$E_{cl} = \frac{E}{D} \tag{6}$$

Where E is the energy absorbed and D is the diameter of the main tube.

Figure 16 displays a bar chart of the various performance indicators used to describe the behaviour of the nested systems.

Upon examination of this figure, it can be seen that all nested systems exhibit similar magnitudes of work effectiveness ranging from 1170 to 1370 [J/kg]. In terms of energy efficiency, it can be seen that the NTCO experienced the highest efficiency of approximately 50% whilst the NTDC experienced the least efficiency of 30%.

Figure 16 illustrates also the energy absorbed per unit crush length (E_{cl}) of nested systems, where the NTCO showed the greatest E_{cl} followed by the NTSC and NTDC respectively. In general, it can be reported that NTCO system exhibited more desirable energy absorption characteristics than NTSC and NTDC systems.

To prove the advantage of using the nested systems as energy absorbing systems for applications with limited crush zones, the E_{cl} was calculated for single circular tube crushed under lateral loading. The circular tube with an outer diameter of 101.6 mm, thickness of 3.25 mm and width of 40 mm was crushed laterally up to 70% of its original diameter. Figure 17 shows the force-deflection response of the single circular tube along with the collapse stages. The E_{cl} was calculated, and it was found to be of approximately 7.5 [J/mm]. This magnitude is approximately half of the Ecl

least magnitude offered by nested systems. So it can be reported that using of the nested tubes system increase the E_{cl} as the nested system has more than one tube deformed simultaneously in the same space.

From the results shown above, it appears that the NTSC system exhibited a superb performance in terms of W_{eff} and SEA.

Also, The NTSC system has a simpler design than NTCO system as it does not need an elongation phase for any of its components. Thus, the NTSC system was selected as the best system between all studied nested tube systems.

To reach the ultimate benefit of this investigation, a parametric study should be performed on the best nested tube system (i.e. NTSC) to generate the design guidelines of such systems. In the following section a parametric study was performed using validated FE models.

3 Numerical simulations and parametric study of the NTSC system

3.1 Finite element modelling

3.1.1 FE model

The finite element models of the NTSC system were constructed using the explicit non-linear finite element code ANSYS-LSDYNA [54]. The FE model consists of the striker, sample, and the base as shown in Figure 18. The samples were modelled by an explicit structural solid element (solid 164), which consists of eight nodes having translations, velocities, and accelerations in the x, y, and z directions at each node. The striker was modelled as a rigid body and constrained to move vertically along the y-axis. The inertia properties and initial velocity of the striker were provided.

The mass defined in the inertia properties of the striker consisted of a carriage mass plus striker mass. The base was also modelled as a rigid entity with all rotations and translations being fixed. An explicit shell element (shell 163) was used to define both striker and base. A fully integrated solid element formulation was used in order to avoid the undesirable hour glassing phenomenon. A 'Plastic Kinematic Hardening' material model was used to define material characterization of the tubes subjected to dynamic loading. Values of 0.3 and 200 [GPa] were employed to define Poisson's ratio and Young's modulus respectively, these values were obtained from the standard tensile test as presented in Table 2. A non-zero value of 1500 MPa was employed to represent the hardening modulus of this material. This value was selected due to limitation of ANSYS-LSDYNA software in defining the softening stage in the bilinear material model, so the value was selected to be as low as possible. The same value of hardening modulus was used by [49, 50] to define the softening stage of the same material. This material model considers strain rate material sensitivity by using the Cowper-Symonds constitutive equation. Values of 6844 and 3.91 were given to D and q respectively. These values were used in previous studies for the axial and lateral crushing of mild steel tubes under dynamic loading [51, 52]. A mesh convergence study was performed to determine the mesh density. It was found that an element size of 2 mm was able to produce a converged solution within a reasonable period of time. Figure 18 shows the half model mesh of the NTSC system.

3.1.2 Validation of FE model

Figure 19 compares the experimental and numerical load-deflection for the NTSC under dynamic loading. The experimental response in Figure 19 corresponds to an impact velocity, V, of 4.5 m/s and an impact mass, M, of 31.45 kg. A slight

discrepancy between the FE and experimental results can be noticed in the post collapse stages. This slight discrepancy is due to the material stress-strain curve used in this study exhibiting an unusual 'material' strain softening phenomenon that is characterised by a negative slope. This type of material behaviour cannot be accounted for in the Plastic Kinematic Hardening material model since it requires that the data points generate a slope greater than zero. Therefore, it is possible that the finite element model's ability to capture the 'material' strain softening phenomenon with sufficient accuracy is limited. However, the FE results are in reasonable agreement with the experimental results.

Of interest for validating simulation results is the deformation mode predicted by the FE code. The deformation modes predicted by the FE code were compared with those from the experiments, as displayed in Figure 20. The prediction given by the FE results for the deformation was excellent. This also supports the validity of the numerical model.

Overall, it is evident that the numerical results predicted by present FE model show good correlation with those from experimental results. This satisfactory agreement indicates that the present FE model is adequate and valid and can be used for the subsequent analyses.

3.2 Parametric study

3.2.1 Effect of geometrical parameters on the system responses

In this section, the effects of geometrical parameters on the energy absorption responses of NTSC system are presented.

The validated FE model as described in section 3.1 was used to perform the parametric study. Our previous investigations on the lateral collapse of thin walled

structures [8-9] revealed that the width of the laterally crushed system has an insignificant effect on the system response particularly on the SEA response. Thus, only the effects of tube diameter and thickness have been considered in this section. Table 4 shows the geometrical variables used to model the NTSC system in the parametric analysis. The range of the geometrical parameters was chosen to cover the typical tube sizes that can be used in crashworthiness applications. Detailed FE models of NTSC were established for the different combinations of geometrical parameters. The numerical tests were conducted under a constant impact velocity of 4.5 [m/sec].

3.2.1.1 Effect of thickness (t)

Figure 21 shows the load-displacement and energy-displacement responses for the NTSC system, as the tubes thicknesses increase for a constant diameter of 150 [mm]. It can clearly be seen that an increase in the wall thickness causes an increase in the load up to a given deflection. This is due to the fact that the greater amount of material across the section of the tube, which effectively increase the lateral stiffness of the tube and hence it requires a greater load to collapse.

Similarly, the energy absorbed up to a given deflection increases as the wall thickness increases. This behaviour is due to the increased amount of material available for plastic deformation and subsequent energy absorption.

3.2.1.2 Effect of Diameter (D)

The effects of varying the tube diameter from 100 [mm] to 150 [mm] were studied for the NTSC system, for a constant tube thicknesses of 2.5 mm. The force-displacement and energy-displacement responses of the NTSC system are depicted in Figure 22 as a function of the tube diameter. From Figure 22(a), it appears that the

crush force decreased as the tube diameter increased. This is due to fact that increasing the tube diameter leads to a decrease in the lateral stiffness of the tube structure, so tubes with bigger diameter need lower collapse forces. The observed effect of the tube diameter on the force-displacement response tubes is also reflected in the energy absorption response, shown in Figure 22(b). It is clear that the energy absorbed up to a given deflection increases with decreasing the tube diameter.

3.2.1.3 Effect of geometrical parameters on other design responses

As mentioned in section 2.4, there are many important responses such as SEA, F, Ecl which give an overall idea about the performance of the structural system as energy absorbing device. Investigating the effects of the geometrical factors on these responses is very beneficial for design purposes.

To gain in-depth understanding of the effect of geometrical factors on these responses, the interaction effects of the studied parameters (i.e. diameter and thickness) on these responses have been considered. In general, the interaction effect occurs when the effect of the first parameter on the response depends on the set of the second parameter.

Specific energy absorption, SEA

SEA is a very important energy absorption indicator, particularly in the structures where weight is of critical importance. To provide a valid comparison of this response, the SEA response for each NTSC system was calculated up to 70% of the diameter (D). This value was carefully selected because it provides a sufficient plastic deformation and enables avoiding undesirable behaviours such as system overloading and extreme plastic strains. Figure 23 presents the interaction effect of D and t on the SEA. It is clear from the figure that the SEA increased with increasing

the tubes thicknesses. This was due to the fact that thicker tubes have more material for plastic deformation. The rate of increase of SEA with thickness, decreased with increasing tube diameter. Also from the same figure, it can be seen that the SEA increased with decreasing the diameter. This was due to localization of plastic strain around the plastic hinges that reduce the volume of material subjected to plastic deformation in the larger tubes. In addition, the increased weight in the larger tubes made the SEA lower.

Collapse load, F

The collapse load (F) is the force required to cause permanent deformation in the system. This response is considered very vital when designing an energy absorbing strictures as the large collapse load often leads to a high deceleration and may cause serious jerking effects or even death to the occupants during an impact.

The interaction effect of diameter and thickness on the collapse load (F) is shown in Figure 24. Clearly, it can be seen that the collapse load increased as the thickness increased. This trend is due to the fact that the NTSC system with thicker tubes has a greater amount of material across the section and thus requires a higher load to initiate lateral collapse of the system.

The effect of thickness on F depends on the diameter and it is more significant in the system with smaller tubes.

The Figure 24 also shows that the crush force decreased with increasing of tube diameter. This behaviour is due to the fact that the smaller tubes have shorter moment arm from the point of load application to the horizontal hinge points. Therefore, a greater magnitude of force was required to initiate the collapse in the smaller tubes.

Energy absorbed per unit crush length, E_{cl}

The high energy absorbed per unit crush length, E_{cl} is the main advantage of the nested tube systems over the others laterally collapse systems. Thus, it is very important to investigate the effects of geometrical parameters on E_{cl}. To provide a valid comparison of this response for each tube, E_{cl} was calculated using the energy absorbed up to a deflection of 70% of the original diameter (D). The interaction effect of t and D on the E_{cl} is plotted in Figure 25. It can be observed from the figure that E_{cl} can be increased by either increasing the tube thickness or decreasing the tube diameter. This is obviously due to the increased energy absorption associated with a lower tube diameter and higher tube thickness. So it can be reported that thicker and smaller tubes are recommended for construction a NTSC system with a higher E_{cl}.

3.2.2 Effect of impact velocity

Of importance for the dynamic analysis of the energy absorption systems is to investigate the behaviour of energy absorbers at high impact velocity. This could not be performed experimentally as the machine has a limited maximum velocity of 4.5 m/sec, so the finite element model was used to simulate the dynamic behaviour of the nested systems and to address the effect of impact velocity the responses of the NTSC system.

Figure 26 illustrates the effect of the impact velocity on the energy absorbed by a NTSC system with an outer diameter of 127 mm, a thickness of 3.25 mm, and a width of 40 mm. This figure plots the energy-deflection responses of the NTSC under different impact velocities. It can be seen that the absorbed energy increased as the impact velocity increased. It also shows that when the impact velocity was less than a certain value, the energy absorbed by the structure was not significantly

affected by the velocity. This is due to fact that the deformation mode of the low impact velocity remains the same as that in the quasi-static case, with a little more plastic deformation localised around the “plastic hinges”. For a high impact velocity (v=100 m/sec), a notable increase in energy absorption was recorded. This behaviour might be due to the inertia effect increased the plastic deformation around the plastic hinges. The Figure 27 shows the numerical collapse sequence of the NTSC system under two different impact velocities. A typical deformation mode was offered by the system under a low impact velocity (v=4. 5 m/Sec). While for v=100 m/sec, the plastic deformation initially occurred near the impact region of the system (upper part of the system), with a little bending deformation in the rest of the system. As the system was further compressed by the upper plate, more plastic deformation was transferred to the other parts of the system. This is evidence that the inertia effect of the dynamic loading becomes more important and significant in the event of high impact velocity.

This observation has been also verified for the other nested tube systems (NTCO and NTDC) as shown in Figure 29 and Figure 30 subsequently.

To further assess the behaviour of the NTSC system under high impact velocity (V=100 m/sec), the energy dissipated by each component of NTSC system was plotted in Figure 28. Upon examination of this figure, it can be seen that the lower small tube did not contribute to the energy dissipation process until the crushing of the upper tube at approximately 40 mm of deflection. This is evidence of the inertia effect with a localised deformation near to the impact region at the beginning of the impact event.

Of interest for dynamic analysis of the NTSC system is to see how the comparison of the dynamic and the quasi-static responses of the energy absorbing component

changed with the velocity of the impinging mass, using the Dynamic Amplification Factor (DAF). This parameter is important for design purposes as it allows the effect of various parameters on the dynamic response to be quantified with respect to the quasi-static response. Based on the calibrated FE model presented in section 5.2.1 5.2.1, Figure 31 which depicts the effect of impact velocity on DAF factor was created. Examination of this figure shows, that an increase in impact velocity caused an increase in the DAF. This was due to an increase in the total internal plastic energy dissipation with an increase of compression velocity. It is clear from Figure 31 that in the range up to a velocity of 30 m/sec, the dynamic effects still did not cause significant variation in the response of the NTSC system, as the DAF magnitude was less than 1.2. Overall, these results are desirable as the impact velocity is an external parameter which is not one of the tube parameters. Thus, the impact velocity has no effect on the system design in the case of low impact velocities (i.e. in the range up to 30 m/sec).

4 Conclusion

The experimental behaviour of the short length nested tube systems under quasi-static and impact lateral loading was presented.

Subsequently, a parametric study was performed, using validated FE model, to investigate the influences of the geometrical and loading parameters on the responses of nested systems. Thus, the design information on using the laterally crushed nested tube systems as energy absorbing structures was generated.

The main points concluded from this paper are drawn as follow

- From the experimental quasi-static analysis, it was found that the nested tube systems NTCO and NTSC exhibited *monotonically increasing* force-deflection responses due to synchronous deformation of all components.
- The NTSC system was very sensitive to geometrical imperfection as any slight difference between the geometries of internal tubes led to *non-monotonic increase* of the force-deflection response.
- From the experimental dynamic analysis, it was found that the magnitude of response from the dynamic cases was similar to their quasi-static counterparts under an experimental velocity of v=4.5 m/sec. It was concluded that this was an indicator of the non-significance of strain rate and inertial effects for the given applied velocity of the striker.
- From the analysis of the performance indicators, it was proof that the nested tube systems can be considered for applications that have a limited crush zone with an increase of energy absorbed per unit length as they have more than one collapsible component in the same space.
- It was found that NTSC system can be selected as the best energy absorption system in the nested systems category due to NTSC showed better energy absorption performance in terms of W_{eff}.
- From the parametric study using the geometrical parameters, it was found that the load-displacement and energy-displacement responses for a NTSC system increased with increasing the tubes thicknesses or decreasing the diameter of the tubes.
- The SEA and E_{cl} for a NTSC system can be maximized by:

  (a) Increasing the thickness of the tubes (t), and/ or

  (b) Decreasing the tube diameter (D)

- The collapse load (F) decreased with decreasing the thickness (t) and/or increasing the tube diameter (D).
- From the parametric study using the impact velocity parameter, it was observed that the energy absorbed by the NTSC system increased with increasing impact velocity. This may be due to the inertia effect increasing plastic deformation around the plastic hinges.
- It was found that at certain velocities, the nested tube systems dissipated the same amount of energy, i.e. the responses were not significantly affected by the velocity of impact. But when the impact velocity was raised above a certain level, the absorbed energy did increase with an increase of impact velocity due to inertia effects. This is evidence of the presence of a critical impact velocity, where under this velocity the dynamic effects on the responses of nested system can be neglected. Further investigation is required to establish the value of this critical velocity.
- Non-symmetrical collapse mode was noticed for all systems in the case of high velocity of the striker, particularly for NTSC and NTCO. This is due to inertia effects that cause localised plastic deformation around the impact region.

Acknowledgment

The first author wishes to gratefully acknowledge the financial support from the University of Aleppo.

References

[1] Olabi, A., Morris, E.and Hashmi, M., (2007), "Metallic tube type energy absorbers: A synopsis", *Thin-Walled Structures,* Vol.45 (7-8), pp. 706-726.

[2] Alghamdi, A.A.A. (2001), "Collapsible impact energy absorbers: an overview", *Thin-Walled Structures,* Vol.39 (2), pp. 189-213.

[3] Abramowicz, W. (2003), "Thin-walled structures as impact energy absorbers", *Thin-walled structures,* Vol.41 (2), pp. 91-107.

[4] Lu, G. and Yu, T., (2003)*, Energy absorption of structures and materials,* , Woodhead Publishing,.

[5] Jones, N., (2011)*, Structural impact,* , Cambridge University Press,.

[6] DeRuntz Jr, J.A.and Hodge Jr, P., (1963), "Crushing of a tube between rigid plates", *Journal of Applied Mechanics,* Vol.30 pp. 391.

[7] Gupta, N., Sekhon, G.and Gupta, P., (2005), "Study of lateral compression of round metallic tubes", *Thin-walled structures,* Vol.43 (6), pp. 895-922.

[8] Baroutaji, A., et al., (2014), “Quasi-static response and multi-objective crashworthiness optimization of oblong tube under lateral loading”, Thin-Walled Structures, Vol.82, pp. 262-277.

[9] Baroutaji, A., et al., (2015), “Crush analysis and multi-objective optimization design for circular tube under quasi-static lateral loading”, Thin-Walled Structures, Vol.86, pp. 121-131.

[10] Yella Reddy, T.and Reid, S., (1979), "Lateral compression of tubes and tube-systems with side constraints", *Int.J.Mech.Sci.,* Vol.21 (3), pp. 187-199.

[11] Reid, S., Drew, S.and Carney III, J., (1983), "Energy absorbing capacities of braced metal tubes", *Int.J.Mech.Sci.,* Vol.25 (9-10), pp. 649-667.

[12] Leu, D.K. (1999), "Finite-element simulation of the lateral compression of aluminium tube between rigid plates", *Int.J.Mech.Sci.,* Vol.41 (6), pp. 621-638.

[13] Gupta, N.and Ray, P., (1998), "Collapse of thin-walled empty and filled square tubes under lateral loading between rigid plates", *International Journal of Crashworthiness,* Vol.3 (3), pp. 265-285.

[14] Sherbourne, A.and Lu, F., (1993), "Strain hardening in the moving hinge method", *Int.J.Solids Structures,* Vol.30 (24), pp. 3475-3489.

[15] Wu, L.and Carney, J.F., (1997), "Initial collapse of braced elliptical tubes under lateral compression", *Int.J.Mech.Sci.,* Vol.39 (9), pp. 1023-1036.

[16] Wu, L.and Carney, J.F., (1998), "Experimental analyses of collapse behaviors of braced elliptical tubes under lateral compression", *Int.J.Mech.Sci.,* Vol.40 (8), pp. 761-777.

[17] Baroutaji, A. and Olabi, A.G., (2012) "Analysis of the Effect of the Elliptical Ratio in Tubular Energy Absorbers Under Quasi-Static Conditions." In *Materials with Complex Behaviour II*, pp. 323-336. Springer Berlin Heidelberg.

[18] Sowerby, R., Johnson, W.and Samanta, S., (1968), "The diametral compression of circular rings by point loads", *Int.J.Mech.Sci.,* Vol.10 (5), pp. 369-370.

[19] Jing, Y.Y.and Barton, D.C., (1998), "The response of square cross-section tubes under lateral impact loading", *International Journal of Crashworthiness,* Vol.3 (4), pp. 359-378.

[20] Thomas, S., Reid, S.and Johnson, W., (1976), "Large deformations of thin-walled circular tubes under transverse loading--I:: An experimental survey of the bending of simply supported tubes under a central load", *Int.J.Mech.Sci.,* Vol.18 (6), pp. 325-326, in3-in6, 327-333.

[21] Watson, A., et al., (1976), "Large deformations of thin-walled circular tubes under transverse loading--II:: Experimental study of the crushing of circular tubes by centrally applied opposed wedge-shaped indenters", *Int.J.Mech.Sci.,* Vol.18 (7-8), pp. 387-388, IN11-IN14, 389-397.

[22] Watson, A., Reid, S.and Johnson, W., (1976), "Large deformations of thin-walled circular tubes under transverse loading—III: Further experiments on the bending of simply supported tubes", *Int.J.Mech.Sci.,* Vol.18 (9), pp. 501-502.

[23] Reid, S.and Bell, W., (1982), "Influence of strain hardening on the deformation of thin rings subjected to opposed concentrated loads", *Int.J.Solids Structures,* Vol.18 (8), pp. 643-658.

[24] Lu, G. (1993), "A study of the crushing of tubes by two indenters", *Int.J.Mech.Sci.,* Vol.35 (3-4), pp. 267-278.

[25] Liu, K., et al., (2005), "Dynamic behavior of ring systems subjected to pulse loading", *Int.J.Impact Eng.,* Vol.31 (10), pp. 1209-1222.

[26] Shim, V.P.W.and Stronge, W., (1986), "Lateral crushing of thin-walled tubes between cylindrical indenters", *Int.J.Mech.Sci.,* Vol.28 (10), pp. 683-707.

[27] Wierzbicki, T.and Suh, M., (1988), "Indentation of tubes under combined loading", *Int.J.Mech.Sci.,* Vol.30 (3-4), pp. 229-248.

[28] Reid, S. (1993), "Plastic deformation mechanisms in axially compressed metal tubes used as impact energy absorbers", *Int.J.Mech.Sci.,* Vol.35 (12), pp. 1035-1052.

[29] Guillow, S., Lu, G.and Grzebieta, R., (2001), "Quasi-static axial compression of thin-walled circular aluminium tubes", *Int.J.Mech.Sci.,* Vol.43 (9), pp. 2103-2123.

[30] Wang, B.and Lu, G., (2002), "Mushrooming of circular tubes under dynamic axial loading", *Thin-walled structures,* Vol.40 (2), pp. 167-182.

[31] Zeinoddini, M., Parke, G.and Harding, J., (2002), "Axially pre-loaded steel tubes subjected to lateral impacts: an experimental study", *Int.J.Impact Eng.,* Vol.27 (6), pp. 669-690.

[32] Rossi, A., Fawaz, Z.and Behdinan, K., (2005), "Numerical simulation of the axial collapse of thin-walled polygonal section tubes", *Thin-walled structures,* Vol.43 (10), pp. 1646-1661.

[33] Nagel, G.and Thambiratnam, D., (2004), "A numerical study on the impact response and energy absorption of tapered thin-walled tubes", *Int.J.Mech.Sci.,* Vol.46 (2), pp. 201-216.

[34] Nagel, G.and Thambiratnam, D., (2005), "Computer simulation and energy absorption of tapered thin-walled rectangular tubes", *Thin-walled structures,* Vol.43 (8), pp. 1225-1242.

[35] Nagel, G.and Thambiratnam, D., (2004), "Dynamic simulation and energy absorption of tapered tubes under impact loading", *International Journal of Crashworthiness,* Vol.9 (4), pp. 389-399.

[36] Gupta, N.and Gupta, S., (1993), "Effect of annealing, size and cut-outs on axial collapse behaviour of circular tubes", *Int.J.Mech.Sci.,* Vol.35 (7), pp. 597-613.

[37] Zhang, X.and Zhang, H., (2013), "Energy absorption of multi-cell stub columns under axial compression", *Thin-Walled Structures,* Vol.68 pp. 156-163.

[38] Reid, S.and Harrigan, J., (1998), "Transient effects in the quasi-static and dynamic internal inversion and nosing of metal tubes", *Int.J.Mech.Sci.,* Vol.40 (2-3), pp. 263-280.

[39] Miscow F, P.and Al-Qureshi, H., (1997), "Mechanics of static and dynamic inversion processes", *Int.J.Mech.Sci.,* Vol.39 (2), pp. 147-161.

[40] Reddy, T.and Reid, S., (1986), "Axial splitting of circular metal tubes", *Int.J.Mech.Sci.,* Vol.28 (2), pp. 111-131.

[41] Lu, G., et al., (1994), "An experimental study on tearing energy in splitting square metal tubes", *Int.J.Mech.Sci.,* Vol.36 (12), pp. 1087-1097.

[42] Jiang, P., Wang, W.and Zhang, G., (2006), "Size effects in the axial tearing of circular tubes during quasi-static and impact loadings", *Int.J.Impact Eng.,* Vol.32 (12), pp. 2048-2065.

[43] Stronge, W., Yu, T.and Johnson, W., (1983), "Long stroke energy dissipation in splitting tubes", *Int.J.Mech.Sci.,* Vol.25 (9-10), pp. 637-647.

[44] Huang, X., Lu, G.and Yu, T.X., (2002), "Energy absorption in splitting square metal tubes", *Thin-walled structures,* Vol.40 (2), pp. 153-165.

[45] Huang, X., Lu, G.and Yu, T.X., (2002), "On the axial splitting and curling of circular metal tubes", *Int.J.Mech.Sci.,* Vol.44 (11), pp. 2369-2391.

[46] Fan, Z., et al., (2012), "Dynamic lateral crushing of empty and sandwich tubes", *Int.J.Impact Eng.,* .

[47] Baroutaji, A., et al. "Analysis and optimization of sandwich tubes energy absorbers under lateral loading." International Journal of Impact Engineering(2015), Article in press, http://dx.doi.org/10.1016/j.ijimpeng.2015.01.005.

[48] Baroutaji, Ahmad, and Abdul-Ghani Olabi. "Lateral collapse of short length sandwich tubes compressed by different indenters and exposed to external constraints." Materialwissenschaft und Werkstofftechnik 45.5 (2014).

[49] Morris, E., Olabi, A.and Hashmi, M., (2007), "Lateral crushing of circular and non-circular tube systems under quasi-static conditions", *Journal of Materials Processing Tech.,* Vol.191 (1-3), pp. 132-135.

[50] Morris, E., Olabi, A.and Hashmi, M., (2006), "Analysis of nested tube type energy absorbers with different indenters and exterior constraints", *Thin-Walled Structures,* Vol.44 (8), pp. 872-885.

[51] Olabi, A., et al., (2008), "Optimised design of nested oblong tube energy absorbers under lateral impact loading", *Int.J.Impact Eng.,* Vol.35 (1), pp. 10-26.

[52] Olabi, A., et al., (2008), "Optimised design of nested circular tube energy absorbers under lateral impact loading", *Int.J.Mech.Sci.,* Vol.50 (1), pp. 104-116.

[53] Wang, Haibo, et al. "Internally nested circular tube system subjected to lateral impact loading." Thin-Walled Structures 91 (2015): 72-81.

[54] ANSYS® Academic Research, Release 14.0, Help System, ANSYS LS-DYNA User's Guide, ANSYS, Inc. 2009

Figure 1: Schematic of a nested tubes sample tube under quasi-static load.

Figure 2: Zwick Roell 5HV series used to conduct the impact experiments.

Figure 3: (a)- The tensile test set-up (b)- True stress–strain curves obtained from three tensile tests .

Figure 1: Schematic of a nested tubes sample tube under quasi-static load.

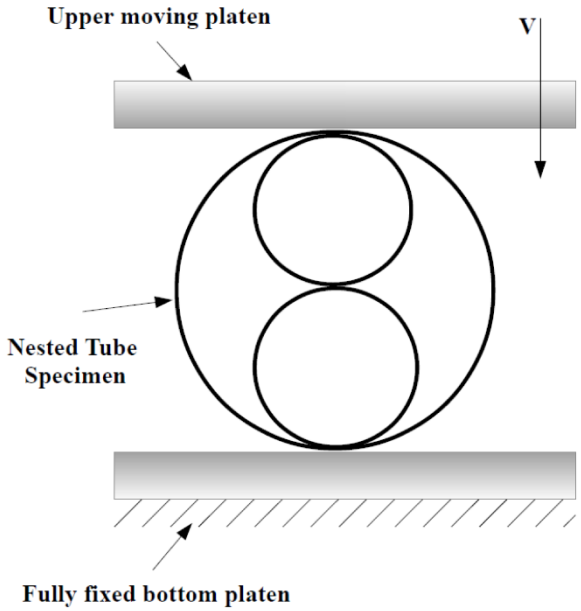

Figure 2: Zwick Roell 5HV series used to conduct the impact experiments.

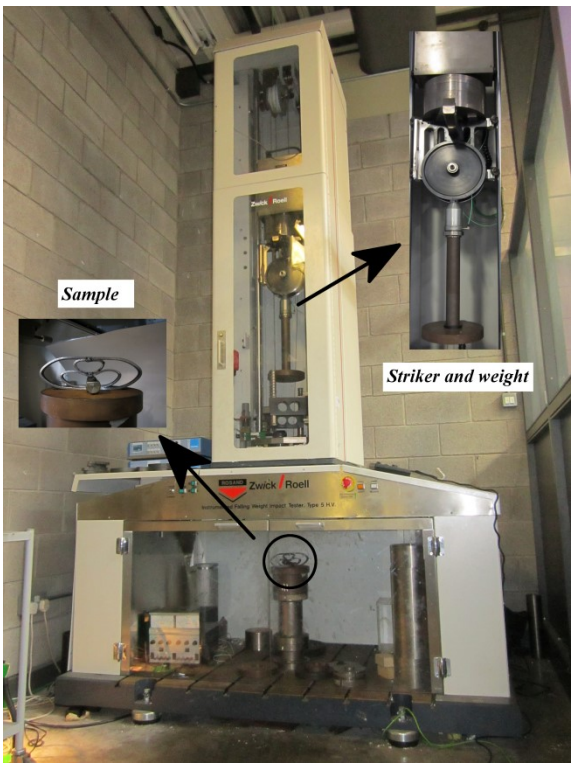

Figure 3: (a)- The tensile test set-up (b)- True stress–strain curves obtained from three tensile tests .

(a)

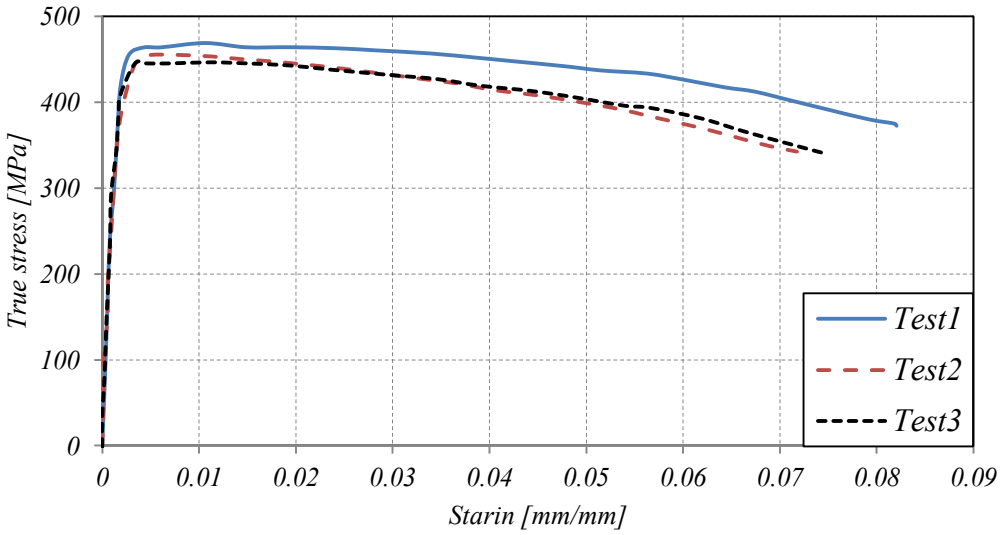

(b)

Figure 4: Experimental responses of a NTCO system

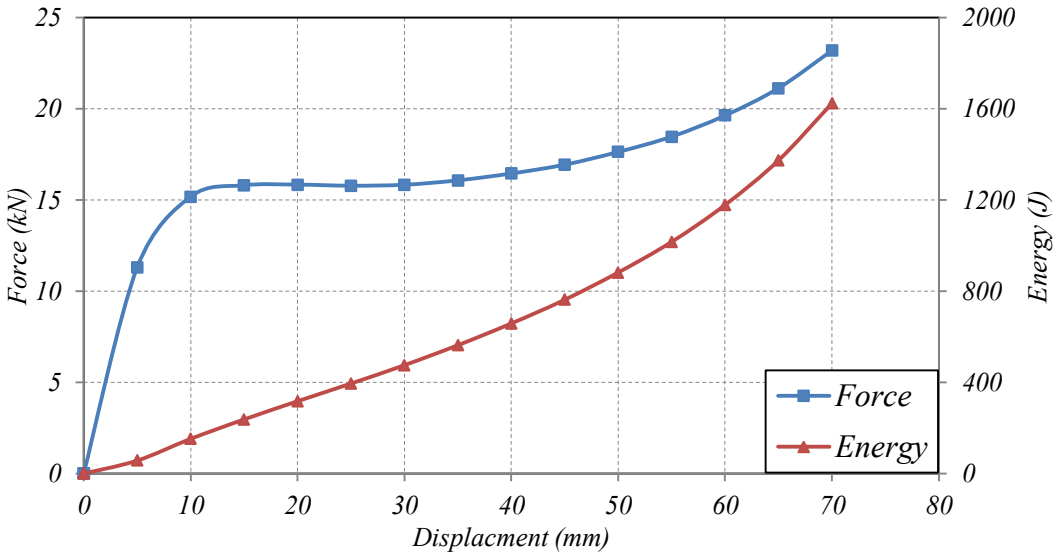

Figure 5: Deformation history of a NTCO system.

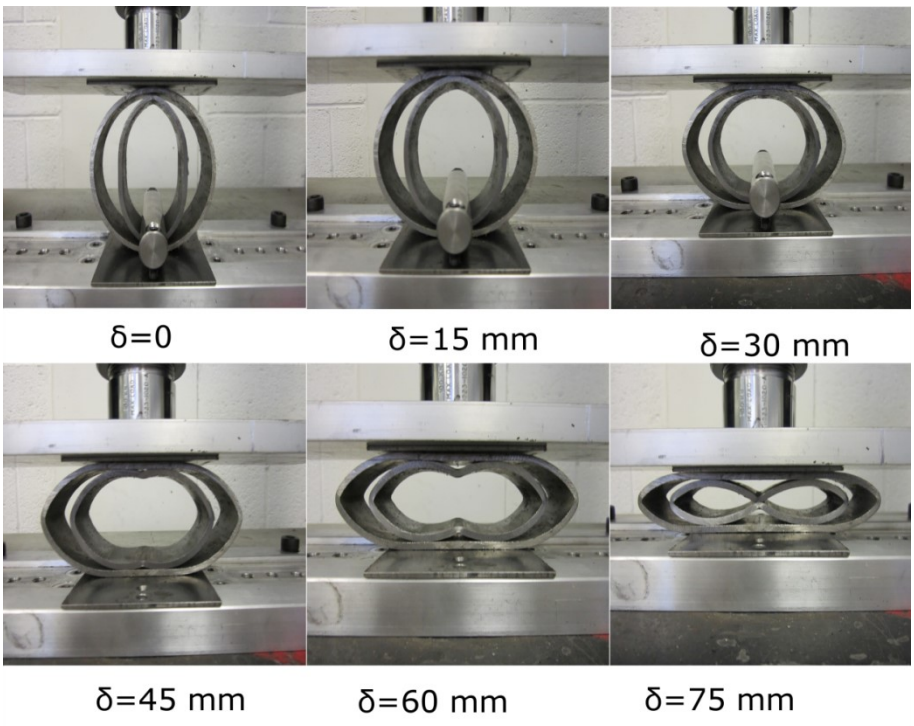

Figure 6: Force and energy responses of the NTDC system.

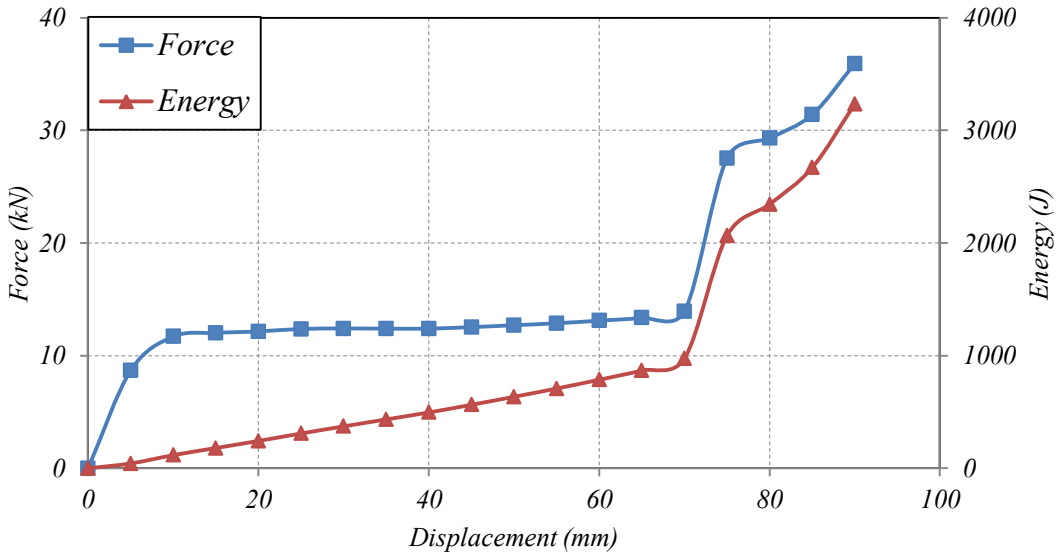

Figure 7: Deformation history of the NTDC system.

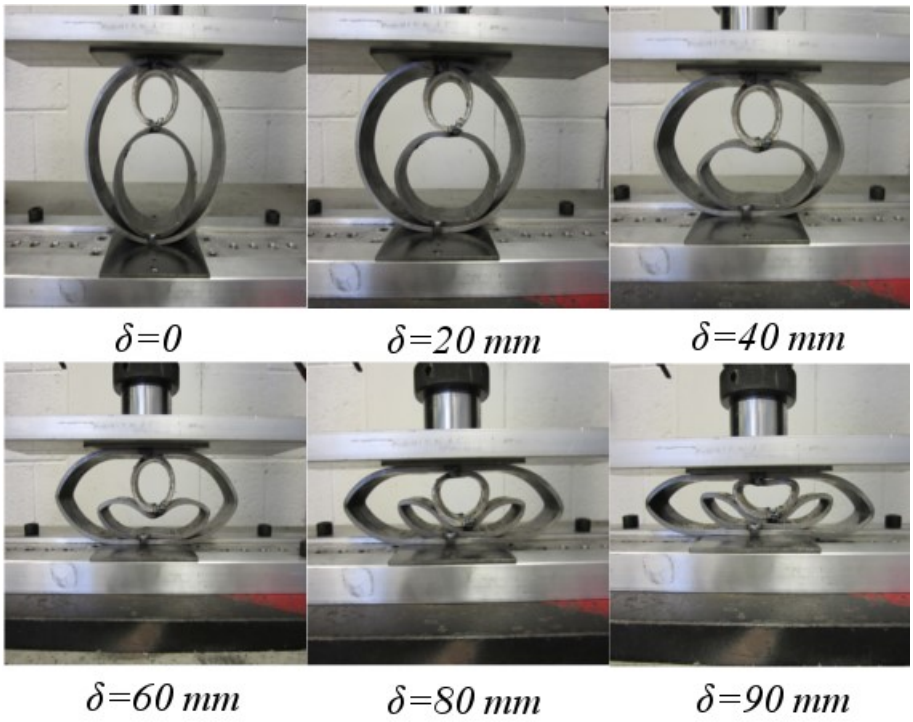

Figure 8: Force and energy responses of the NTSC system.

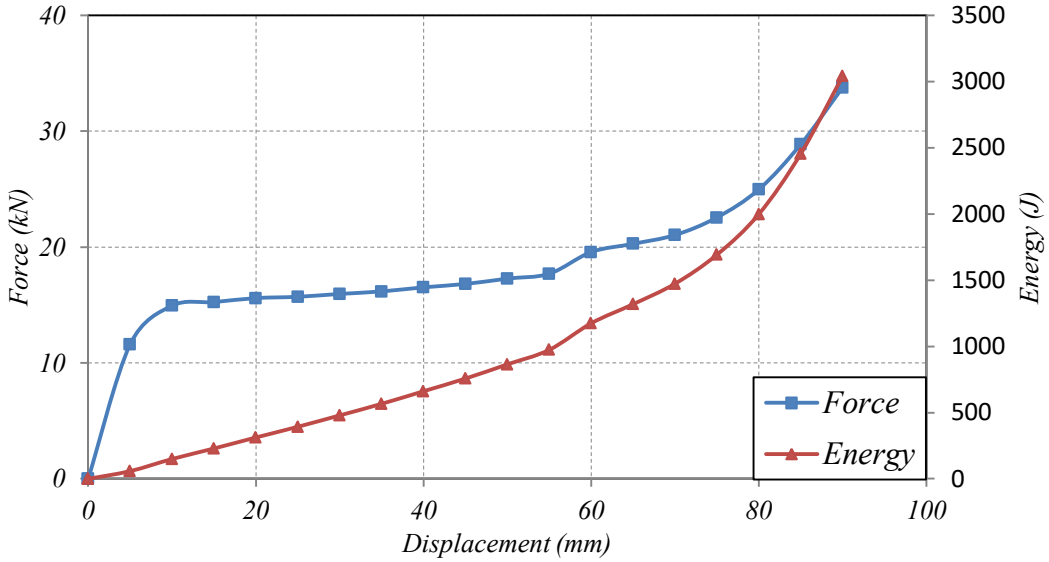

Figure 9: Deformation history of the NTSC system.

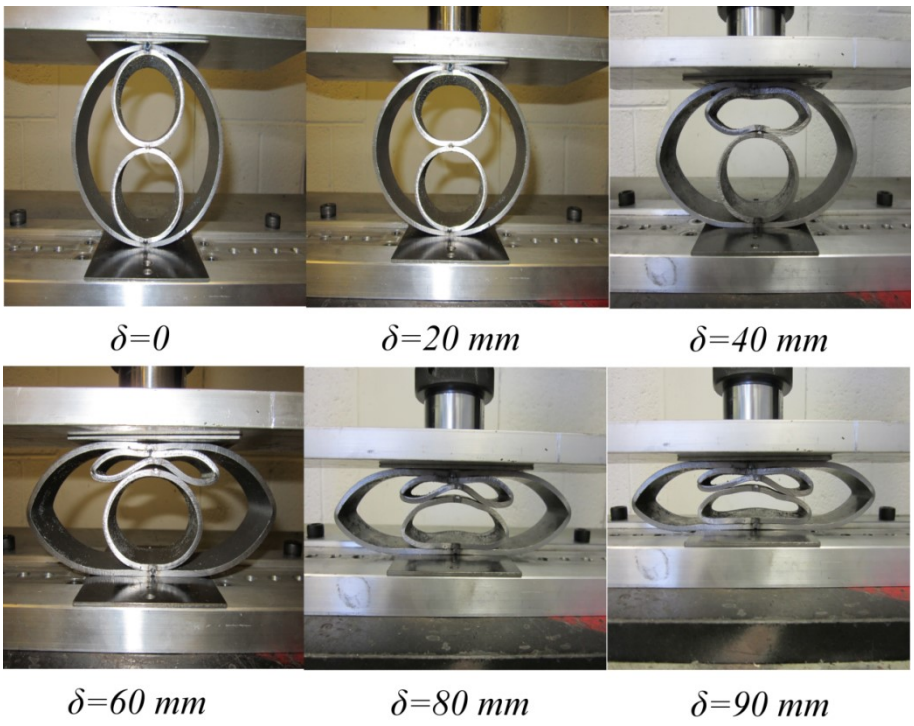

Figure 10: Comparison of load-displacement curves of the NTCO system for quasi-static and dynamic crushing (v=4.5 m/sec).

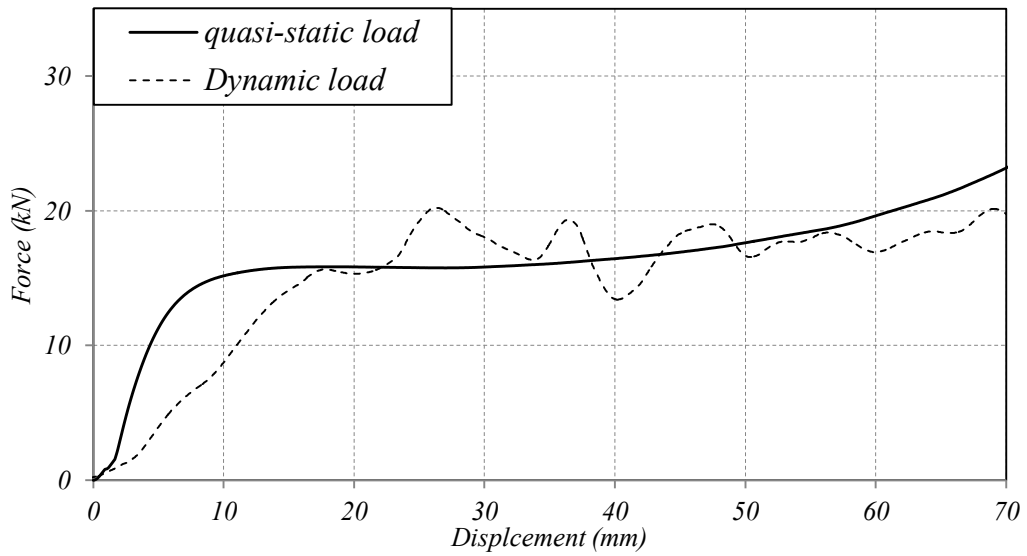

Figure 11: a- initial, and b- final stages of NTCO under dynamic loading.

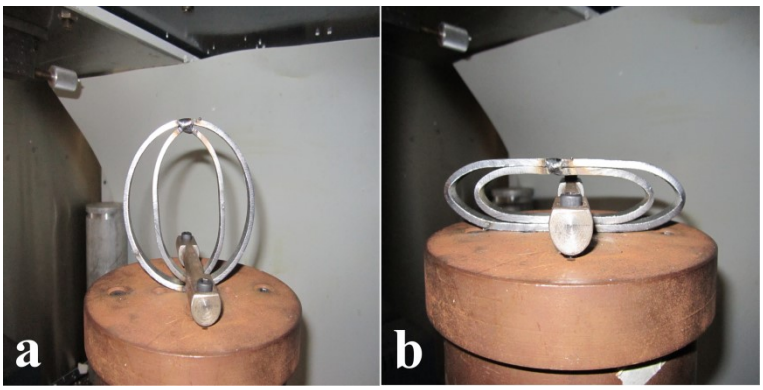

Figure 12: Comparison of load-displacement curves for the NTDC system for quasi-static and dynamic crushing (v=4.5 m/sec)

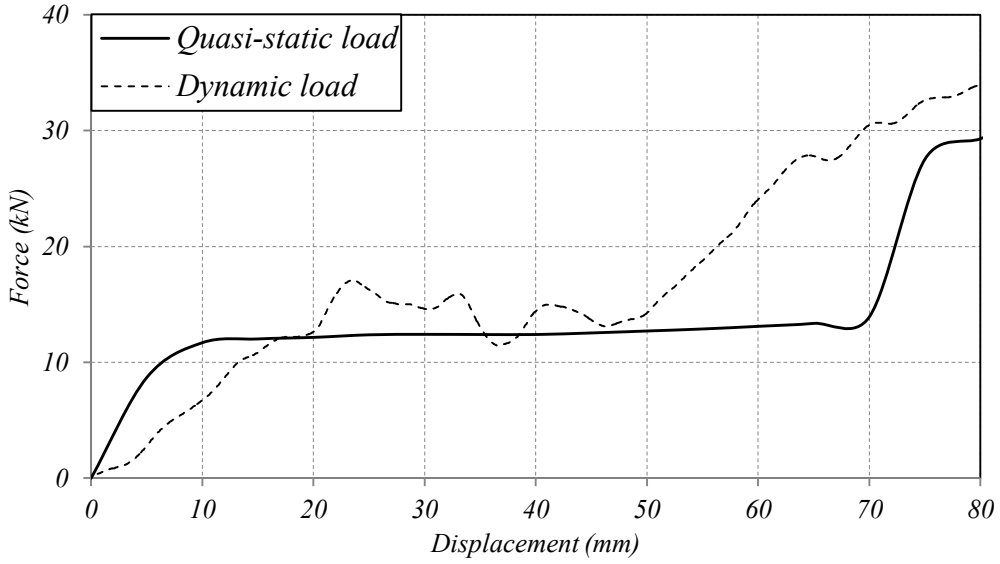

Figure 13: a- initial, and b- final stages of the NTDC under dynamic loading

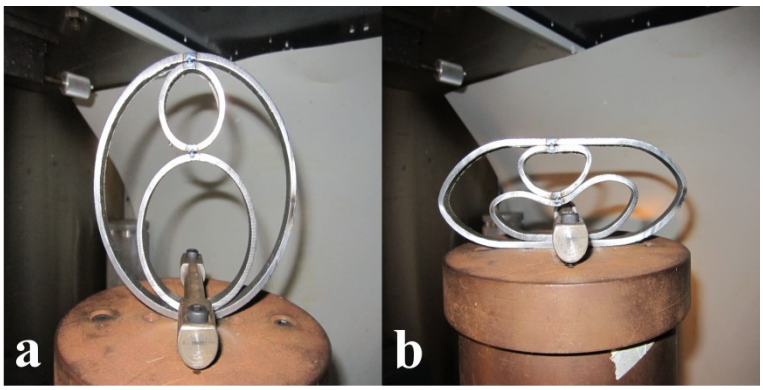

Figure 14: Comparison of the quasi-static and dynamic crushing load-displacement curves for the NTSC system (v=4.5 m/sec).

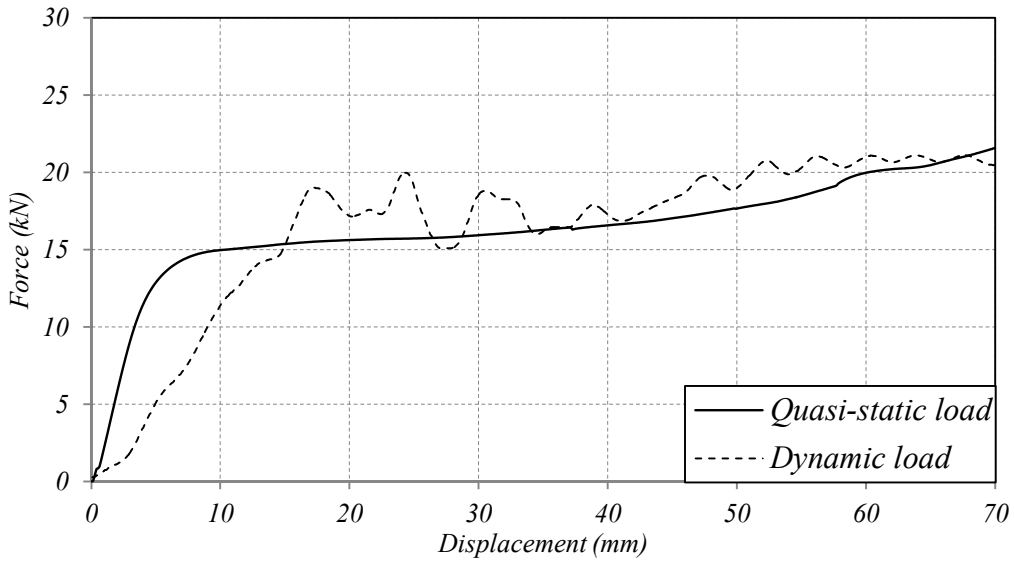

Figure 15: a- initial, and b- final stages of NTSC under dynamic loading.

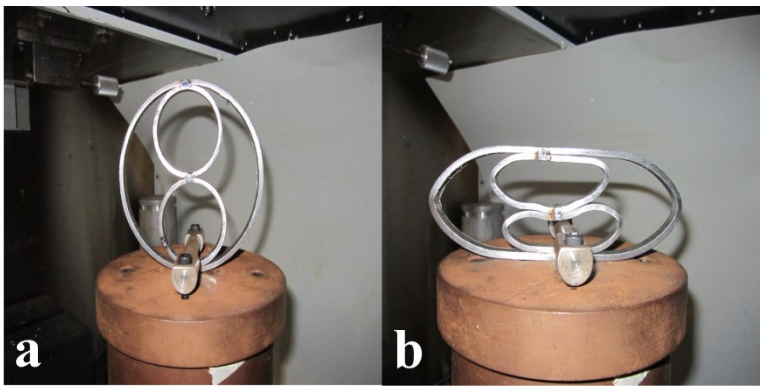

Figure 16: Performance characteristics of nested systems.

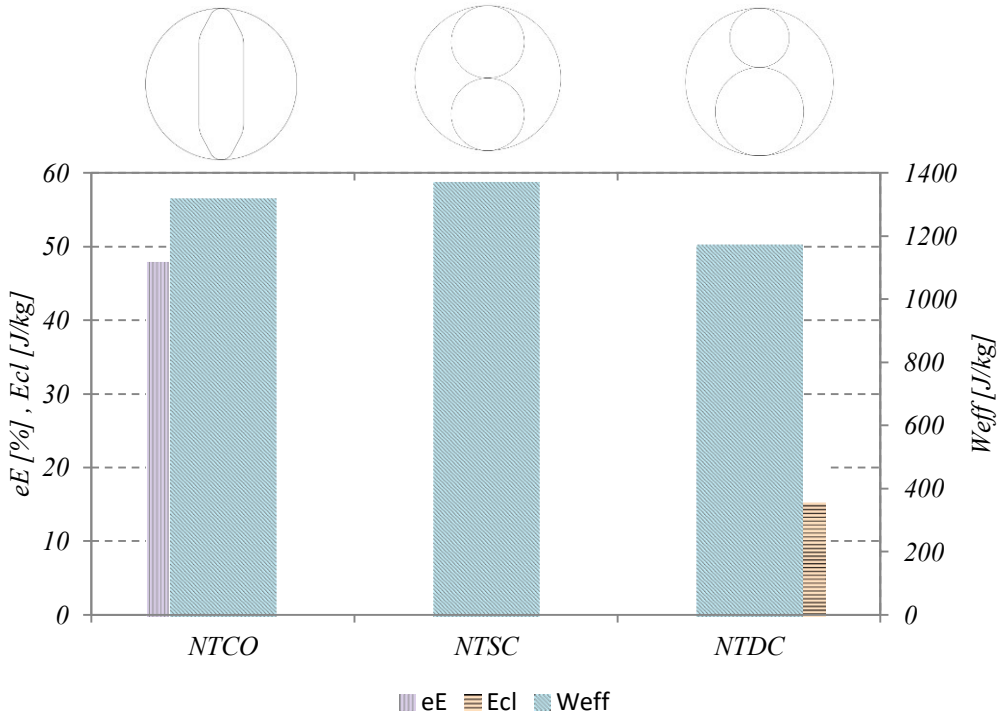

Figure 17: Force -deflection response of single circular tube under lateral loading.

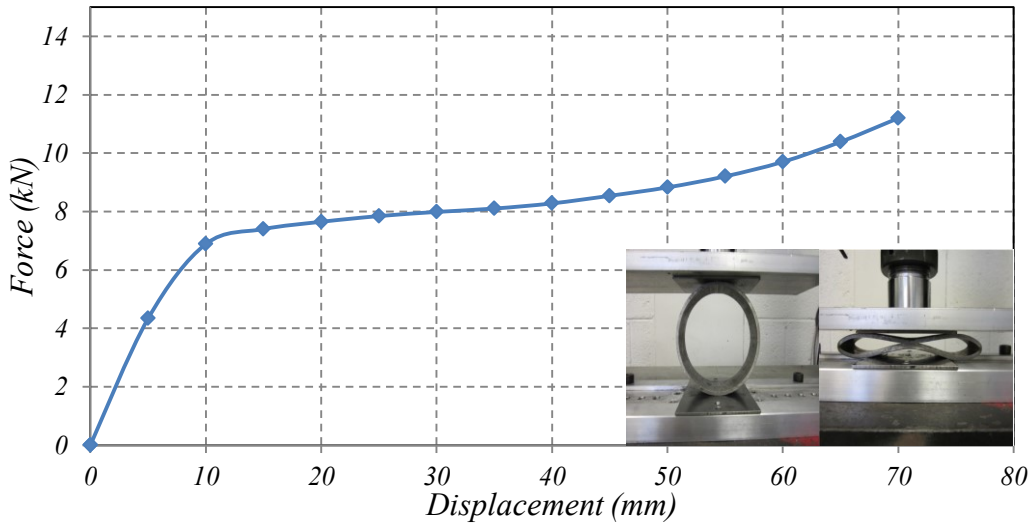

Figure 18: FE model of NTSC system.

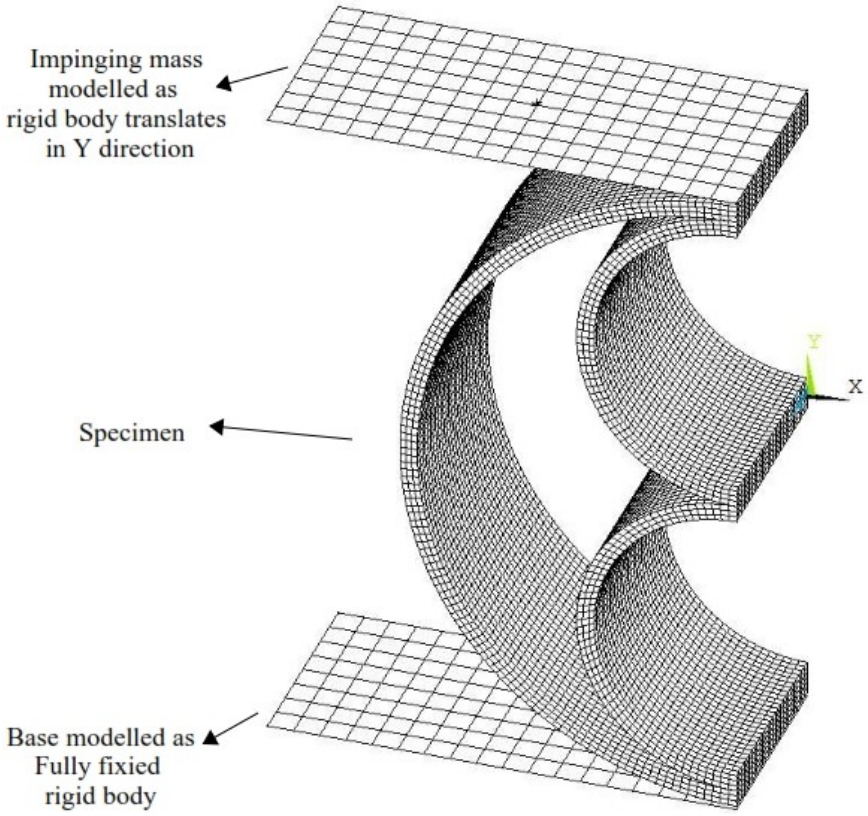

Figure 19: Comparison of FE & experimental results for a nested tube system under dynamic loading (v=4.5 m/sec).

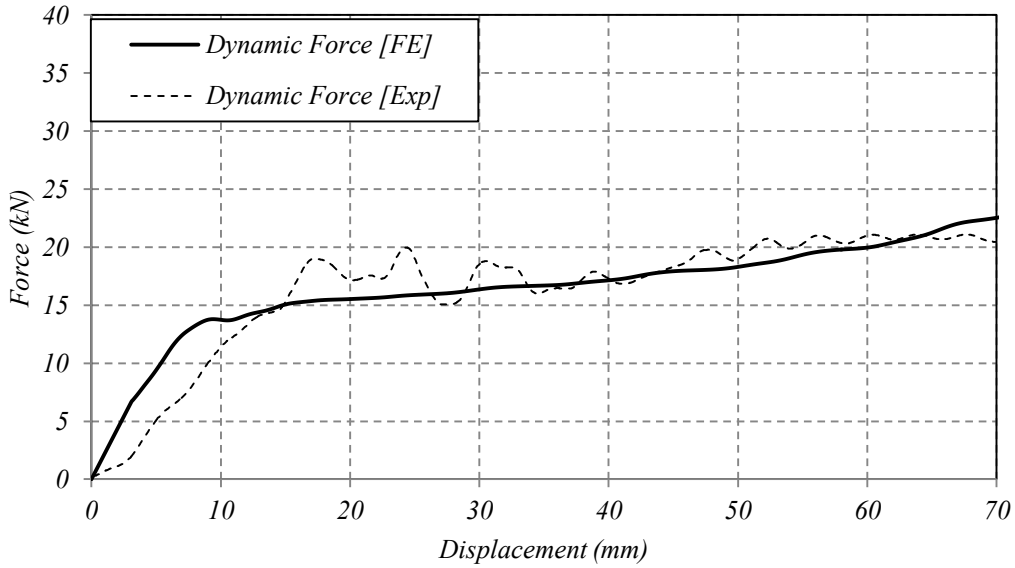

Figure 20: Comparison of (a) the experimental and (b) the numerical deformation mode of nested tubes.

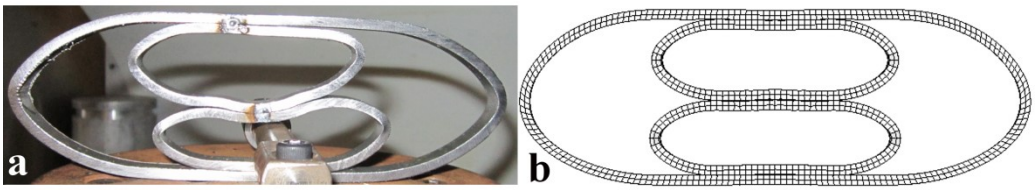

Figure 21: Effect of tube thickness (D) on (a) Force-displacement response, (b) absorbed energy- displacement response. (here D=150 mm)

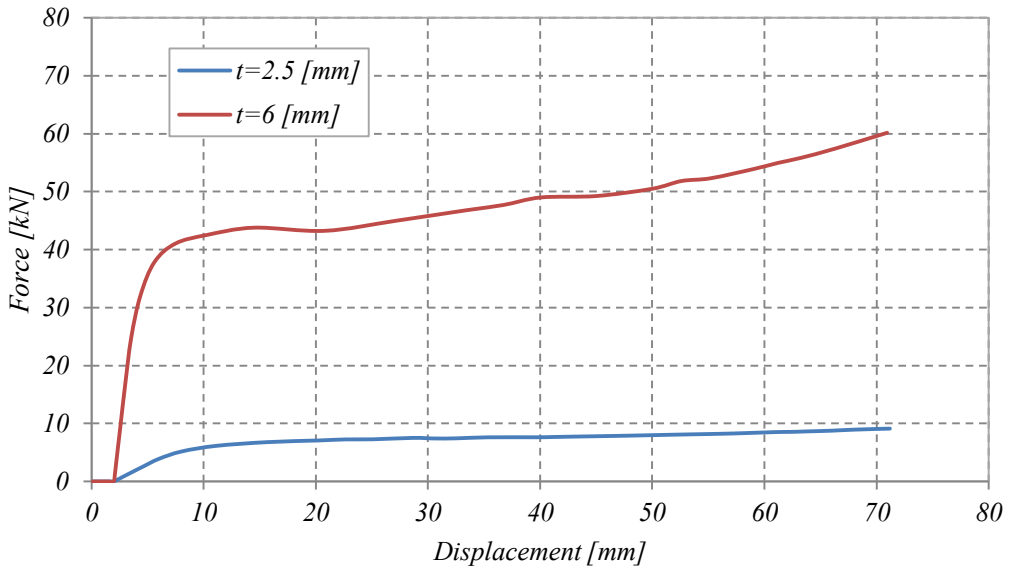

(a)

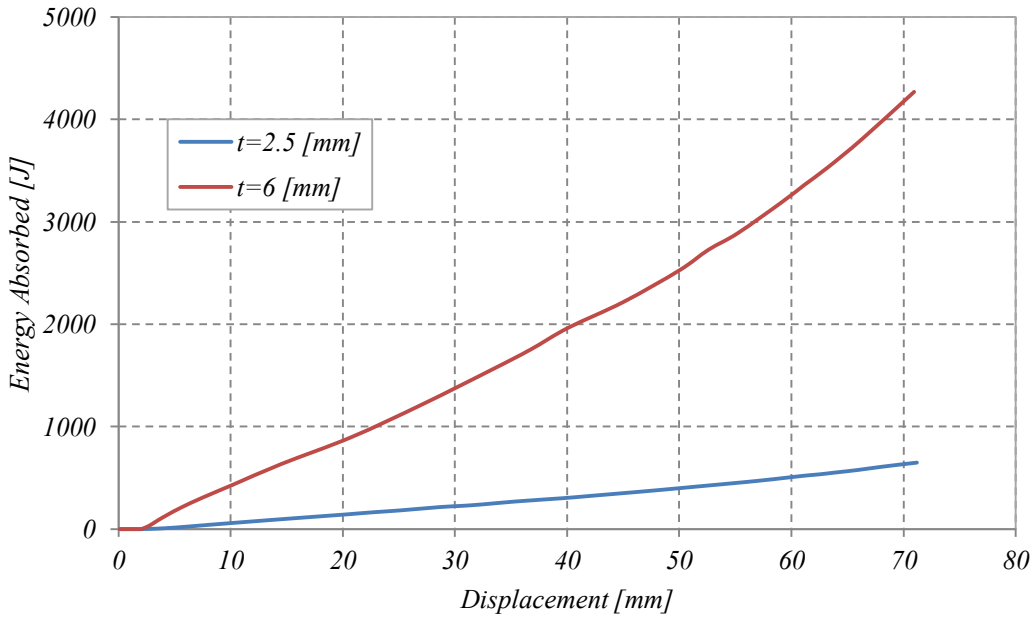

(b)

Figure 22: Effect of tube diameter (D) on (a) Force-displacement response, (b) Aborbed energy- displacement response. (here t=2.5 mm)

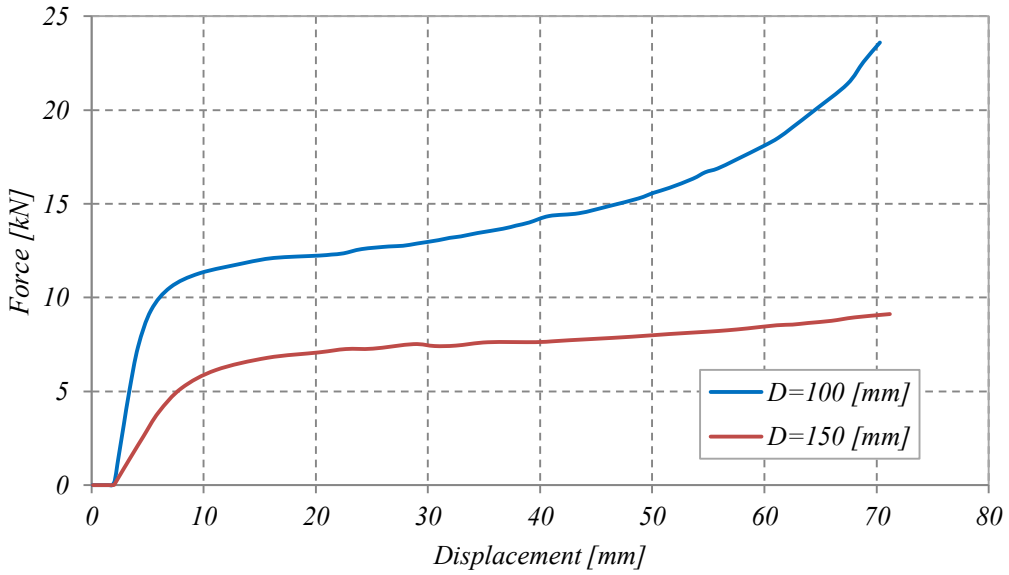

(a)

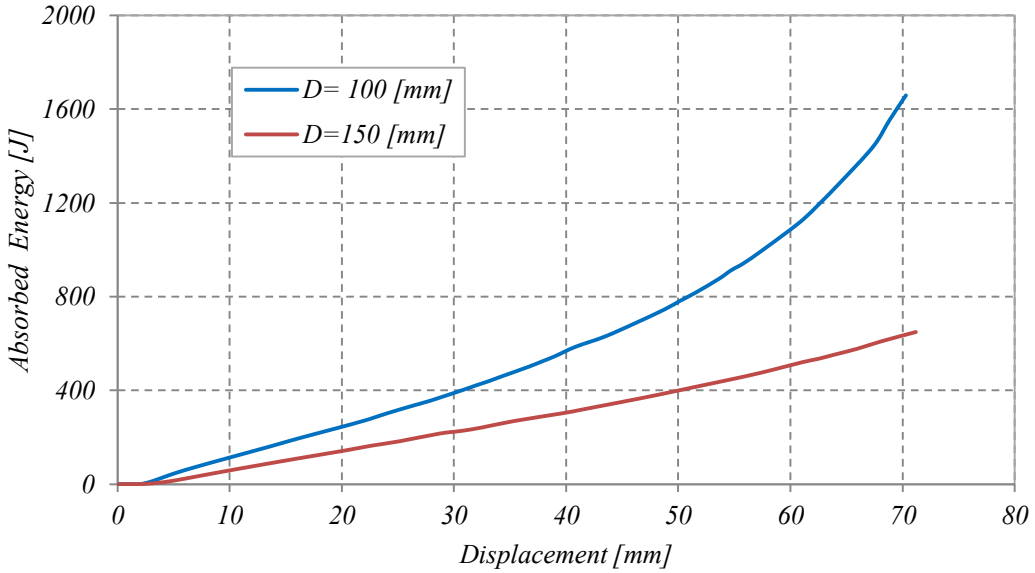

(b)

Figure 23: Interaction effect of D and t on the SEA

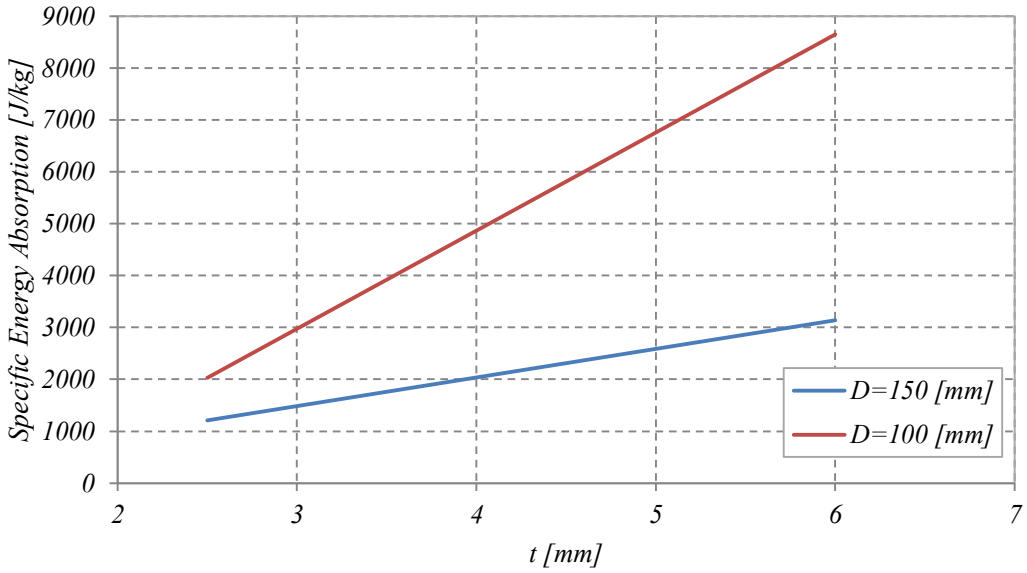

Figure 24: Interaction effect of D and t on the F

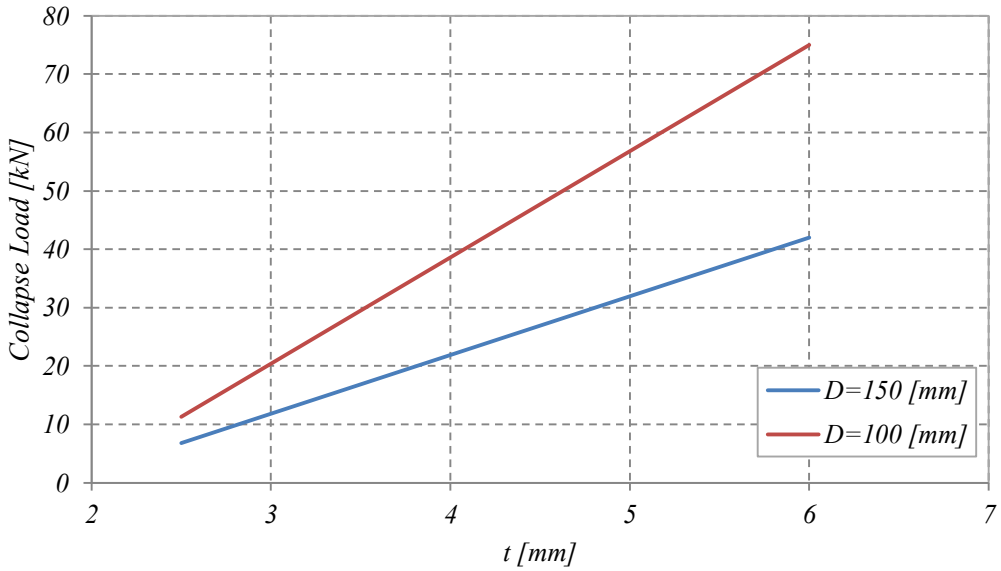

Figure 25: Interaction effect of D and t on the E_{cl}

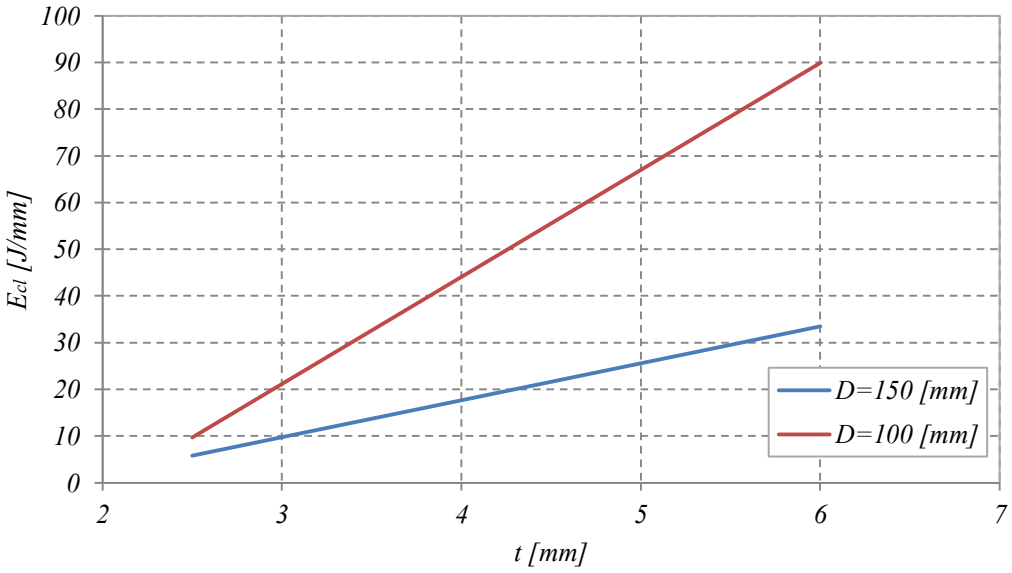

Figure 26: Energy-deflection responses of the NTSC system under different impact velocities.

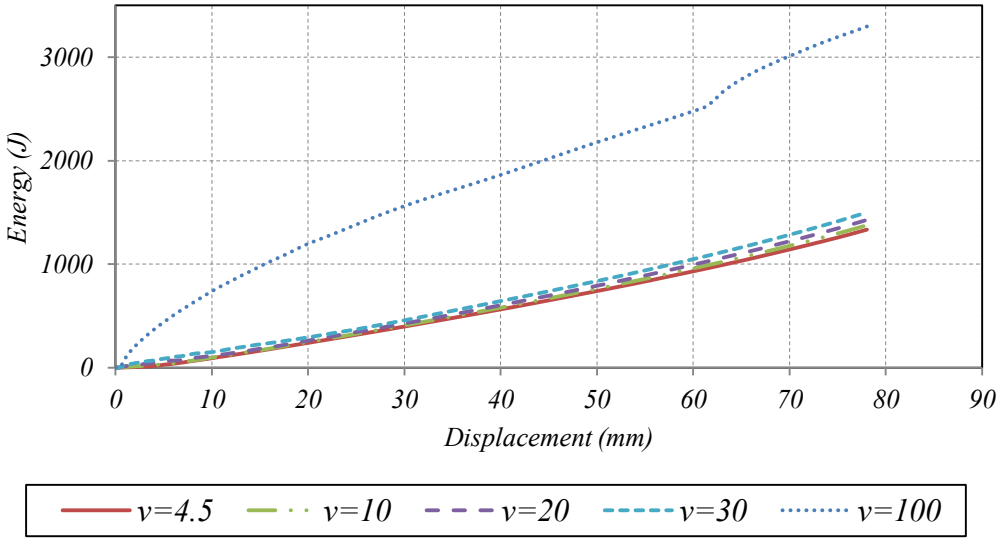

Figure 27: Deformation profiles of the NTSC system under two different impact velocity, a: v=10 m/sec, and b: v=100 m/sec.

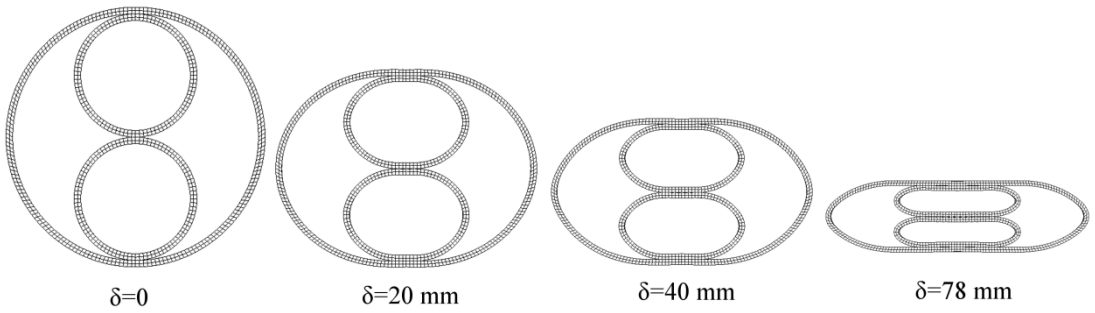

a

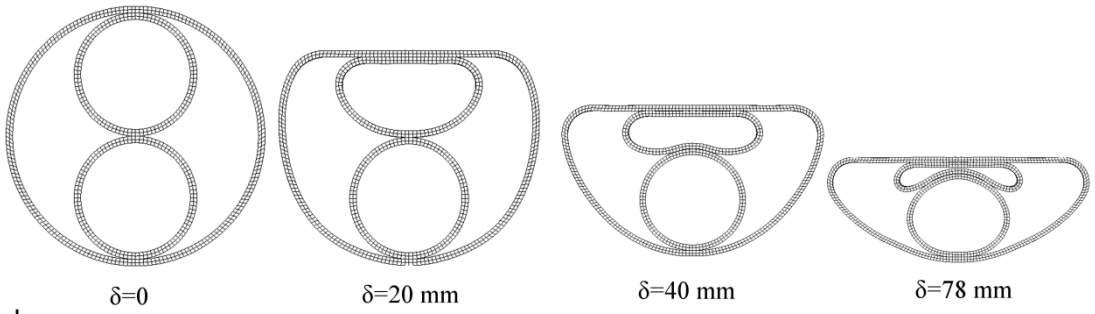

b

Figure 28: Energy-displacement responses for each component of the NTSC system under an impact velocity of 100 m/sec where e_1 is the energy absorbed by main tube, e_2 is energy absorbed by upper tube and e_3 is the energy absorbed by the lower tube.

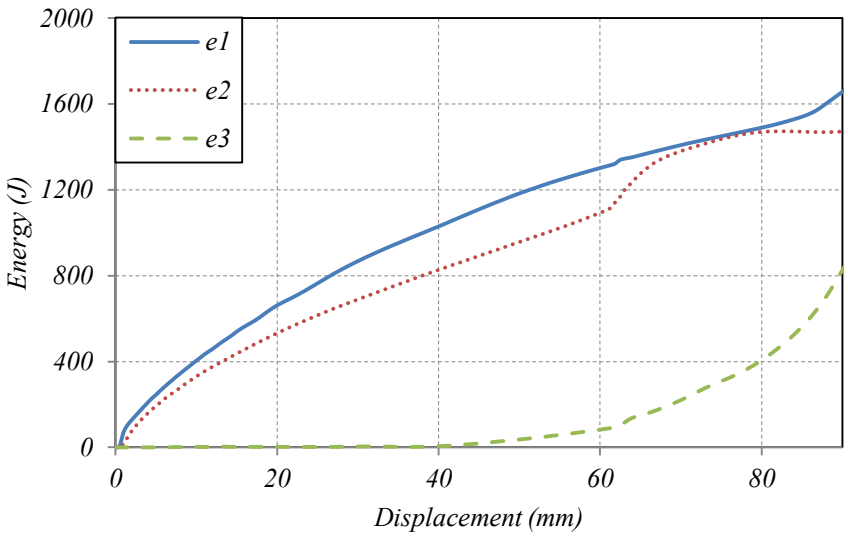

Figure 29: predicted Deformed profiles of the NCOT system under two different compression velocity a: v=10m/sec, and b: v=100 m/sec.

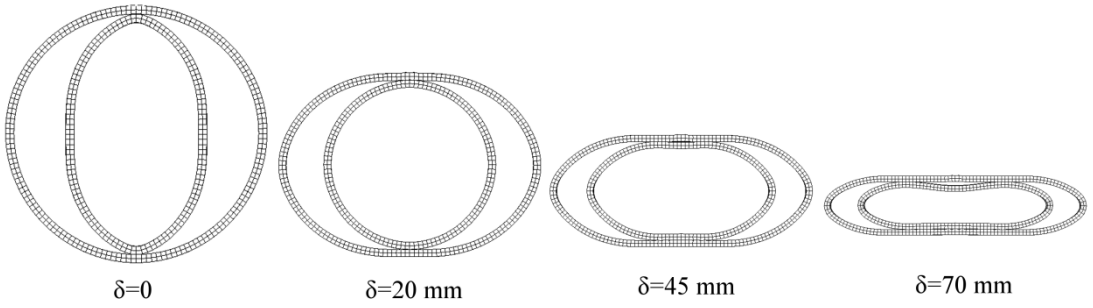

a

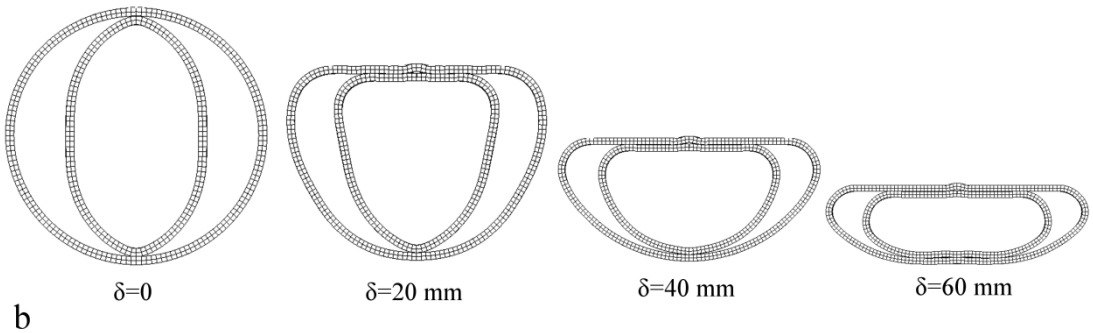

b

Figure 30: Deformation profiles of the NTDC system under two different compression velocity a- v=10m/sec and b- v=100 m/sec

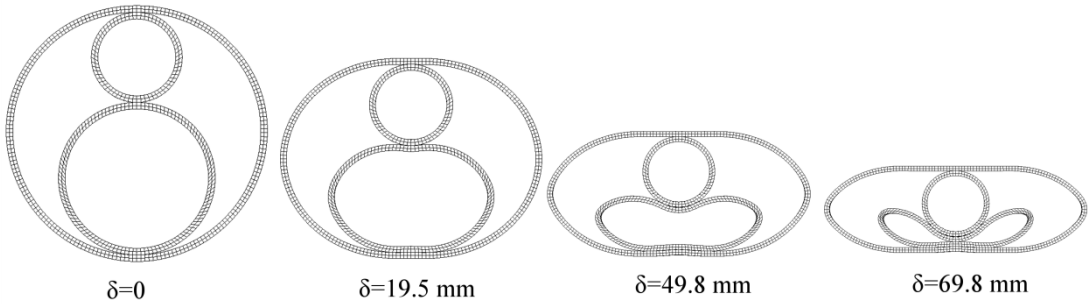

a

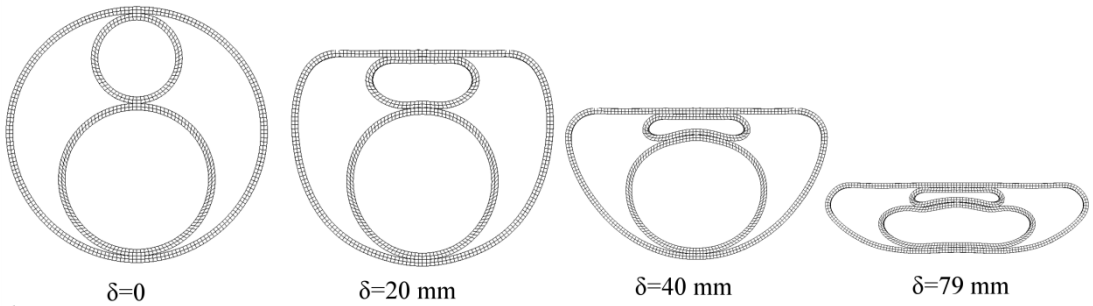

b

Figure 31: Effect of impact velocity on the *DAF*.

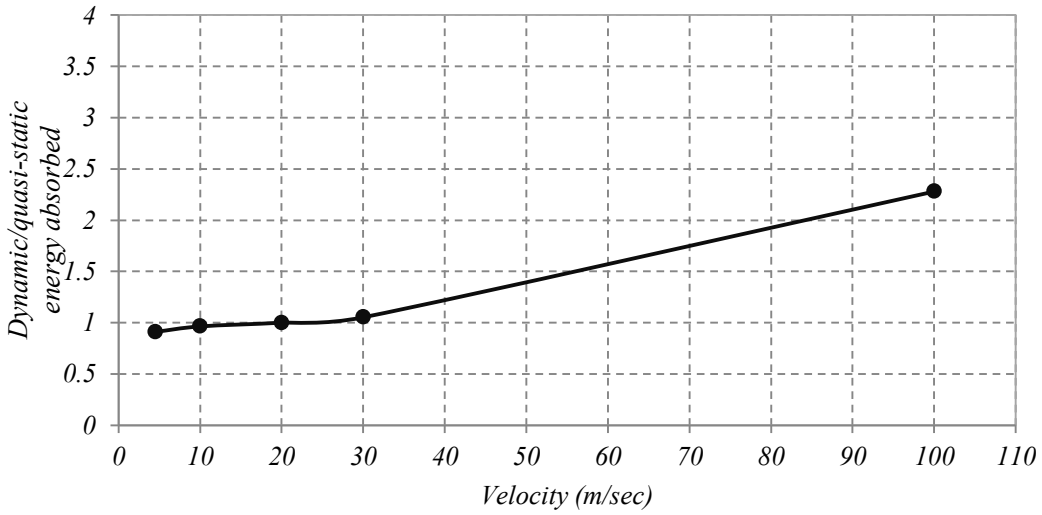

Table 1: Chemical Composition of steel tubes (obtained from supplier)

	C % (max)	*Si % (max)*	*Mn % (max)*	*P % (max)*	*S %*
DIN 2393 ST 37.2	0.17	0.35	0.7	0.05	0.05

Table 2: Material properties of empty and nested tubes

	Density (kg/m3)	*Young's modulus (GPa)*	*Poisson's ratio*	*Yield strength Rp0.2 (MPa)*
DIN 2393-ST 37.2	7861	200	0.3	470

Table 3: Configurations and dimensions of nested tube systems

Geometry	*Dimensions*	*Abbreviations*
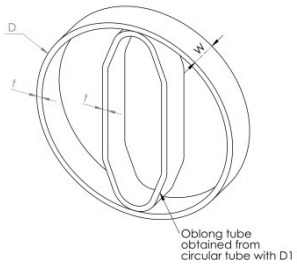	D=101.6[mm]-t=3.25[mm] D1=76[mm]-W=40[mm]	NTCO
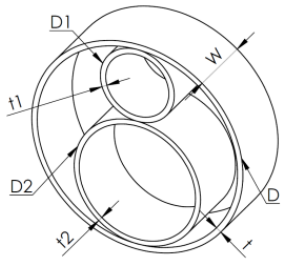	D=127[mm]-t=3.25[mm] D1=41[mm]-t1=3.25[mm] D2=76[mm]-t2=3.25[mm] W=40[mm]	NTDC
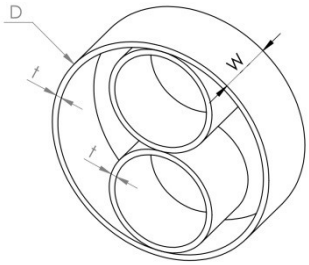	D=127[mm]-t=3.25[mm] W=40[mm]	NTSC

Table 4: Model dimensions used in the parametric analysis of NTSC system

T (mm)	D (mm)	W (mm)
2.5	100	40
2.5	150	40
6	150	40
6	100	40